ISSN 1063-7834, Physics of the Solid State, 2012, Vol. 54, No. 1, pp. 143–154. © Pleiades Publishing, Ltd., 2012.
Original Russian Text © M.S. Molokeev, S.V. Misyul', 2012, published in Fizika Tverdogo Tela, 2012, Vol. 54, No. 1, pp. 134–143.

PHASE TRANSITIONS

Structural Changes during Phase Transitions and the Critical and Noncritical Order Parameters in the $(NH_4)_3Nb(O_2)_2F_4$ Crystal

M. S. Molokeev[a, *] and S. V. Misyul'[b]

[a] *Kirensky Institute of Physics, Siberian Branch of the Russian Academy of Sciences, Akademgorodok 50–38, Krasnoyarsk, 660036 Russia*

* *e-mail: msmolokeev@mail.ru*

[b] *Siberian Federal University, Svobodnyi pr. 79, Krasnoyarsk, 660041 Russia*

Received May 31, 2011

Abstract—The structures of two phases of the $(NH_4)_3Nb(O_2)_2F_4$ crystal, namely, the parent cubic phase and the most distorted low-temperature phase, have been determined from data of an X-ray diffraction experiment performed for a powder sample. The profile and structural parameters have been refined according to the procedure implemented in the DDM program. The results obtained have been discussed with invoking the group-theoretical analysis of the complete order parameter condensate, which takes into account the critical and noncritical atomic displacements and allows the interpretation of the obtained experimental data. It has been found that the most probable sequence of structural transformations occurring in the crystal can be schematically represented in the following form:

$$Fm\bar{3}m \xrightarrow[(\eta 1, \eta 1, \eta)]{\Gamma_5^+(11-7)} C2/m \xrightarrow[(\eta 1, \eta 1, \eta)(0, 0, 0, 0, 0, \xi, 0, -\xi, 0, 0, 0, 0)]{\Gamma_5^+(11-7)\otimes\Sigma_2(4-2)} P2_1/m$$

$$\xrightarrow[(\eta 1, \eta 1, \eta)(0, 0, 0, 0, 0, \xi, 0, -\xi, 0, 0, 0, 0)(0, 0, 0, 0, 0, \varepsilon, 0, \varepsilon, 0, 0, 0, 0)]{\Gamma_5^+(11-7)\otimes\Sigma_2(4-2)\otimes\Sigma_3(4-3)} P2_1/n.$$

DOI: 10.1134/S1063783412010234

1. INTRODUCTION

The specific features of the structure of compounds with the general formula $A_2BMO_xF_{6-x}$ (where A, B = K, Rb, Cs; M = Ti, Mo, W; x = 1, 2, 3) have been repeatedly reported in the literature [1, 2] and, in particular, in our previous papers [3–5]. It is especially important that the main structural elements in these compounds are noncentrosymmetric oxyfluoride anions MO_xF_{6-x}, which, under specific conditions, allow the formation of polar structures with ferroelectric properties [3]. However, the majority of fluorine–oxygen compounds crystallize in the nonpolar phase of the cubic elpasolite-like structure with a face-centered lattice (space group $Fm\bar{3}m$, $Z = 4$), which, most likely, indicates a fluorine–oxygen disorder in the MO_xF_{6-x} anions. With a decrease in the temperature, the majority of the oxyfluorides undergo phase transitions of the ferroelastic or ferroelectric nature due to the processes of ordering and small displacements of atoms [3–5].

An attempt to determine the structures of the compounds $(NH_4)_3Nb(O_2)_2F_4$ and $(NH_4)_3Ta(O_2)_2F_4$ with the cubic symmetry $Fm\bar{3}m$ ($Z = 4$) at room temperature was made by Ružić-Toroš et al. [6]. According to the data obtained by those authors, in the parent cubic phase of these compounds, the fluorine atoms are located in the position 24*e* and disordered over six positions, whereas the oxygen atoms are located in the position 96*j* and distributed over 24 positions. However, in such compounds, the oxygen atoms form dumbbell-like groups $(O–O)^{2-}$. Therefore, it is more expedient to speak about the (O_2) group rather than about a single oxygen atom. Then, the center of mass of the (O_2) dumbbell is located in the position 24*e* and distributed over 12 positions.

Unfortunately, in [6], a number of questions remained open. In particular, the coordinates of the hydrogen atoms of the ammonium groups were not determined and the geometry of the $Nb(O_2)_2F_4$ polyhedron was not elucidated. Furthermore, in the aforementioned paper, the authors presented a figure with the cis location of peroxide groups in the $Nb(O_2)_2F_4$ polyhedron, which is in contradiction with the vibrational spectra obtained by Von Schmidt et al. [7] for the $(NH_4)_3Ta(O_2)_2F_4$ compound. Reasoning only from the information on the structures of the cubic phases of the $(NH_4)_3Nb(O_2)_2F_4$ and $(NH_4)_3Ta(O_2)_2F_4$ compounds, which were determined in [6], one can construct several variants of the location of the (O_2)

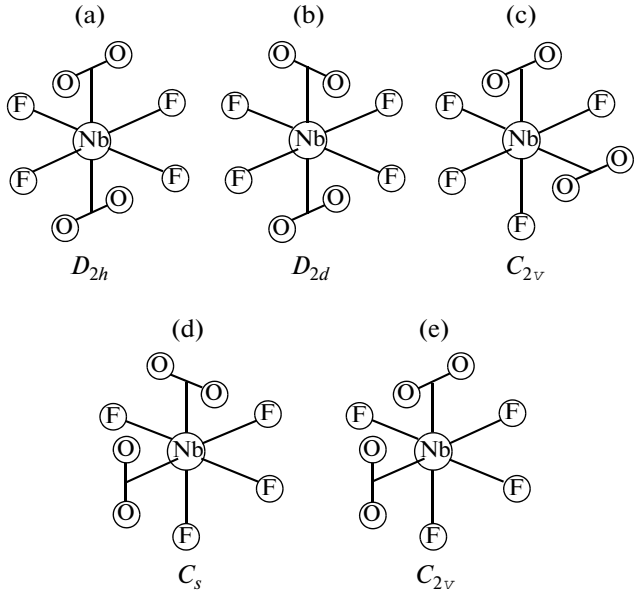

Fig. 1. (a–e) Variants of the arrangement of the molecular groups (O_2) in the $Nb(O_2)_2F_4$ polyhedron of the cubic phase of the $(NH_4)_3Nb(O_2)_2F_4$ crystal.

dumbbells in the $Nb(O_2)_2F_4$ polyhedron (Fig. 1); however, none of them can be preferred.

Recently, Fokina et al. [8] carried out calorimetric investigations of the phase transitions in the $(NH_4)_3Nb(O_2)_2F_4$ compound and, from the changes observed in the heat capacity during cooling of the samples, revealed the occurrence of three adjacent first-order structural transformations at close temperatures: $T_1 = 193.0$ K, $T_2 = 187.2$ K, and $T_3 = 185.4$ K. It was found that, during heating of the samples, the peaks corresponding to the revealed anomalies in the heat capacity at the phase transition points merge into a single peak. Since the temperatures of the phase transitions were close to each other, the authors managed to determine only the total entropy of the phase transitions, which was evaluated as $\Delta S_1 + \Delta S_2 + \Delta S_3 = R\ln 20$, where ΔS_1, ΔS_2, and ΔS_3 are the entropies of the phase transitions at temperatures T_1, T_2, and T_3, respectively. Such a high value of the total entropy suggests that, in the crystal, there occur processes of ordering of the $Nb(O_2)_2F_4$ groups and tetrahedral ammonium ions. Judging from the shape of the anomalies revealed in the heat capacity in [8], one can also argue that the maximum contribution to the orderings observed in the structure under consideration comes from the processes occurring in the first phase transition ($T_1 = 193.0$ K).

In order to elucidate the mechanism of the phase transformations occurring in the $(NH_4)_3Nb(O_2)_2F_4$ crystal and to eliminate the discrepancies revealed in the previous studies of this material, we carried out more accurate temperature X-ray powder diffraction investigations of the structural characteristics of the crystal and their changes during the phase transitions observed in this crystal.

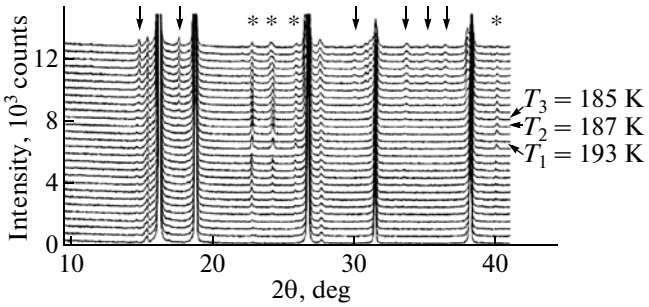

Fig. 2. Fragments of the X-ray diffraction patterns of the $(NH_4)_3Nb(O_2)_2F_4$ compound measured at temperatures varying from 155 to 253 K in steps of 2 K. The arrows indicate the superstructure reflections, and the asterisks denote the reflections obtained from the ice phase.

2. SAMPLE PREPARATION AND EXPERIMENTAL TECHNIQUE

Niobium oxyfluoride $(NH_4)_3Nb(O_2)_2F_4$ was synthesized in the form of a white crystalline powder by the solution crystallization method.

The X-ray diffraction patterns from polycrystalline samples of the $(NH_4)_3Nb(O_2)_2F_4$ compound were recorded using an Anton Paar TTK450 temperature chamber installed on a D8-ADVANCE X-ray powder diffractometer (Cu$K\alpha$ radiation, θ–2θ scan mode, VANTEC linear position-sensitive detector). Liquid nitrogen was used as a coolant. The scan step in the angle 2θ was equal to 0.016°, and exposure per frame was 0.3 s. The experiments were carried out at temperatures in the range from 155 to 253 K with a step of 2 K. This made it possible to reveal regularities in the variations of the structural characteristics of the crystal during the phase transition. In order to more reliably refine the structures of the parent phase G_0 and the distorted phase G_3 at two temperatures (298 and 133 K), each being fairly different from the phase transition temperatures, the exposure at each experimental step was increased to 0.6 s. The temperatures of the chosen experiments excluded the influence of transient phenomena.

3. EXPERIMENTAL RESULTS

It can be seen from Figs. 2 and 3 that, as the temperature decreases after the first phase transition at the temperature $T_1 = 193.0$ K, the shape of the X-ray diffraction pattern taken from the powdered sample of the $(NH_4)_3Nb(O_2)_2F_4$ compound remains almost unchanged. In these X-ray diffraction patterns, there are no superstructure reflections or a noticeable split-

ting of the principal reflections. There exists only an insignificant broadening of some peaks. Furthermore, we could reliably establish neither a splitting of the peaks nor superstructure reflections during cooling of the sample after the second phase transition within a narrow temperature range between $T_2 = 187.2$ K and $T_3 = 185.4$ K.

Below the temperature of the third phase transition ($T_3 = 185$ K), the X-ray diffraction patterns of the $(NH_4)_3Nb(O_2)_2F_4$ compound are characterized by a clearly pronounced splitting of the principal reflections (Fig. 3), for which the X-ray line diagram is shown in Fig. 4. The form of the splitting (Fig. 4) of the principal reflections from the G_3 phase indicates that the unit cell of this phase has the monoclinic symmetry. Here and further in the text, the indices of all reflections are given in terms of the parameters of the cubic unit cell. By using the homology method [9], the splitting of the principal reflections in the X-ray diffraction patterns can be interpreted as the following most probable sequence of symmetry changes of the phases: cubic phase $G_0 \longrightarrow$ unknown phase $G_1 \longrightarrow$ unknown phase $G_2 \longrightarrow$ monoclinic phase G_3 with the twofold axis along the diagonal of the face of the former cubic unit cell.

At temperatures below $T_3 = 185.4$ K, i.e., in the G_3 phase, a system of superstructure reflections appears in the X-ray diffraction pattern (Fig. 2), and the intensity of these reflections increases with a decrease in the temperature (Fig. 5a). The thermal behavior of the integrated intensity of these reflections enables one to separate them from a small number of clearly pronounced reflections attributed to impurities (Fig. 2). However, the total integrated intensity of the structural reflections decreases with a decrease in the temperature (Fig. 5b), which, as a rule, is associated with the process of redistribution of the integrated intensity between the structural and superstructure reflections.

Our attempts to determine the unit cell parameters of the G_3 phase with the known program ITO [10] have failed for a number of reasons, in particular, because of the large shift of the plane of the sample surface (by $-0.05°$) after cooling of the crystal. In the nearest future, it is planned to publish an article devoted to a detailed description of an original program that makes it possible to properly choose the parameters of the distorted unit cells in accordance with the splitting of the principal reflections and from the comparison of the positions of the superstructure reflections in the X-ray diffraction pattern with the theoretically calculated positions of these reflections.

By using the homology method [9] and the original program for the determination of the point and translational symmetries of the distorted phase, it has been established that only the monoclinic unit cell, which has the parameters $\mathbf{a}_1 = (-\mathbf{a}_0 - \mathbf{c}_0)/2$, $\mathbf{b}_1 = \mathbf{a}_0 - \mathbf{c}_0$, and $\mathbf{c}_1 = -\mathbf{b}_0$ (where $\mathbf{a}_0$, $\mathbf{b}_0$, and $\mathbf{c}_0$ are the fundamental vec-

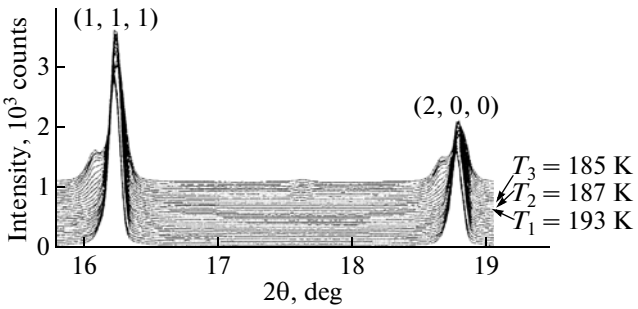

Fig. 3. Fragments of the X-ray diffraction patterns with the reflections (1, 1, 1) and (2, 0, 0) obtained from the $(NH_4)_3Nb(O_2)_2F_4$ compound measured at temperatures varying from 155 to 253 K in steps of 2 K.

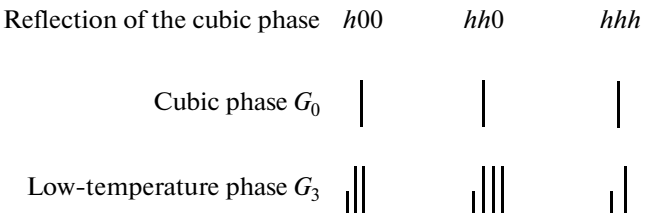

Fig. 4. Splitting of the principal reflections of the cubic phase G_0 of the $(NH_4)_3Nb(O_2)_2F_4$ compound, which are observed in the monoclinic phase G_3.

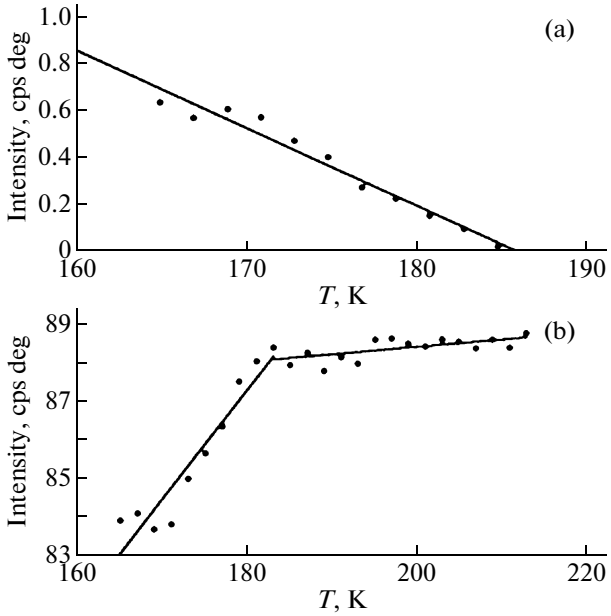

Fig. 5. Temperature dependences of the integrated intensity of (a) the (2, 1, 0) superstructure reflection obtained from the $(NH_4)_3Nb(O_2)_2F_4$ compound and (b) all structural reflections with the Wulff–Bragg angle up to $2\theta = 50°$.

Table 1. Data collection and structure refinement parameters of the $(NH_4)_3Nb(O_2)_2F_4$ compound

Parameter	$T = 298$ K	$T = 133$ K
Space group	$Fm\bar{3}m$	$P2_1/n$
$\mathbf{a}_i$, Å	$\mathbf{a}_0$, 9.43787(6)	$(-\mathbf{a}_0 - \mathbf{c}_0)/2$, 6.6681(3)
$\mathbf{b}_i$, Å	$\mathbf{b}_0$, 9.43787(6)	$\mathbf{a}_0 - \mathbf{c}_0$, 13.2740(5)
$\mathbf{c}_i$, Å	$\mathbf{c}_0$, 9.43787(6)	$-\mathbf{b}_0$, 9.4797(3)
β, deg	90	89.146(2)
V, Å^3	840.66(1)	838.96(5)
Z	4	4
2θ angle range, deg	5–110	5–110
Number of reflections	42	1055
Number of parameters refined	12	45
R_B, %	2.94	3.41
R_{DDM}, %	10.13	14.13

Note: R_B is the Bragg integral discrepancy factor, and R_{DDM} is the profile discrepancy factor determined with the DDM program [11].

tors of the face-centered cubic Bravais cell) and the fourfold volume as compared to the volume of the primitive cubic cell ($V_3/V_0 = 4$, where V_3 and V_0 are the volumes of the primitive cells of the corresponding phases), is suitable for the description of the entire profile of the X-ray diffraction pattern of the distorted phase G_3.

The structural models of the cubic phase G_0 and the distorted phase G_3 were determined using the traditional Patterson function method. The profile and structural parameters were refined according to a new procedure implemented in the DDM program, which has not yet been widely used [11] (Table 1). The shapes of the peaks were described by the Pearson VII function. Figures 6a and 6b illustrate the thermal behavior of the parameters of the reduced cubic unit cell, which were obtained during the fitting of the profiles of the X-ray diffraction patterns with the DDM program. It should be noted that, with a decrease in the temperature, the volume of the cubic unit cell increases abruptly by approximately $100\delta V/V_0 \approx 1\%$ at the temperature $T_3 = 185.4$ K of the phase transition (see Fig. 6c), which indicates a clearly pronounced first-order phase transition.

Knowing the total change in the entropy $\Delta S = R\ln 20$, we can estimate the coefficient that indicates the shift in the phase transition temperature under pressure, dT/dP, according to the following formula: $dT/dP = (\delta V a^3 N_A)/(Z\Delta S) \approx -50.5$ K/GPa, where a is the parameter of the cubic unit cell, N_A is the Avogadro number, and $Z = 4$ is the number of formula units per unit cell. The experimentally measured values of dT/dP [8] were found to be as follows: $(dT/dP)_1 \approx -44$ K/GPa for the first phase transition and $(dT/dP)_2 \approx -57$ K/GPa for the second phase transition. It can be seen that the average value of the experimentally measured quantities dT/dP is close to the calculated value.

In the high-temperature cubic phase G_0 at a temperature of 293 K, the $(NH_4)_3Nb(O_2)_2F_4$ crystal has a cubic cryolite structure (Table 2). The primitive cell contains one Nb atom and two independent ammonium NH_4 groups, one of which is located in the position 4*b* and the other one occupies the position 8*c*. The tetrahedral configuration of the NH_4 ion in the position 4*b* with the octahedral environment requires that the hydrogen atoms should be disordered (Table 2). The hydrogen atoms of the other ammonium ion, which is located in the position 8*c*, have already been ordered in the cubic phase. The oxygen and fluorine atoms of the $N(O_2)_2F_4$ polyhedron are disordered over different regular systems of points of the cubic unit cell. In particular, the fluorine ions occupy the position 24*e* with the occupation multiplicity of the position of 2.3.

Let us consider the positions of the oxygen atoms in more details. The coordinates of the oxygen atoms were refined within the framework of two models: in the first model, the oxygen atom is located in the position 24*e* with the position occupancy of 2/3; and in the second model, the oxygen atom is located in the position 96*j* with the position occupancy of 1.6. In the first model, the coordinates of the oxygen ion were refined with the anisotropic thermal parameters. The discrepancy factor in this approximation was found to be $R_B = 5.35\%$. In the other model with the oxygen atom located in the position 96*j*, after the further refinement of its position in the isotropic approximation, the discrepancy factor drastically decreased to $R_B = 2.94\%$ (Table 2). The correctness of the choice of this model

for the cubic phase is confirmed by the structure of the distorted phase G_3.

Unfortunately, our attempts to establish structures of the intermediate phases G_1 and G_2 have failed because of the narrow temperature region of their existence and the influence of the transition effects in this region.

The experimental data obtained at a temperature of 133 K allowed us to reliably determine the structure of the monoclinic phase G_3 of the $(NH_4)_3Nb(O_2)_2F_4$ crystal. The primitive cell of the G_3 phase contains one independent niobium atom, three independent NH_4 ions, four independent fluorine atoms, and four independent oxygen atoms. All the fluorine and oxygen atoms involved in the $Nb(O_2)_2F_4$ polyhedra are ordered in the G_3 phase. The difference electron density synthesis in the monoclinic phase G_3 has revealed peaks corresponding to four hydrogen atoms around the ammonium ion, which contains the N1 atom and has been disordered in the cubic phase. The N–H bond lengths and the H–N–H bond angles correspond to the geometry of the regular NH_4 tetrahedron. The position of the other ammonium ion, which contains the N2 atom and has already been ordered in the cubic phase, is split in the monoclinic phase G_3 into two positions that correspond to the N2 and N3 atoms (see Table 2). The coordinates of the hydrogen atoms around the N2 and N3 atoms were also found from the positions of the electron density peaks in the difference synthesis. A further refinement of the coordinates of all the atoms involved in the structure within the isotropic approximation led to a low discrepancy factor $R_B = 3.41\%$.

The results of the structure refinement of two phases of the $(NH_4)_3Nb(O_2)_2F_4$ compound are presented in Tables 1 and 2. The selected bond lengths are listed in Table 3. The structures of the cubic and monoclinic phases of the $(NH_4)_3Nb(O_2)_2F_4$ compound are shown in Fig. 7. The geometric parameters of the hydrogen bonds in the $(NH_4)_3Nb(O_2)_2F_4$ structure are given in Table 4. The configuration of the hydrogen bonds in the structure of the $(NH_4)_3Nb(O_2)_2F_4$ compound in the monoclinic phase G_3 is illustrated in Fig. 8. The geometry of the $Nb(O_2)_2F_4$ polyhedron in the monoclinic phase G_3 in two projections is shown in Fig. 9.

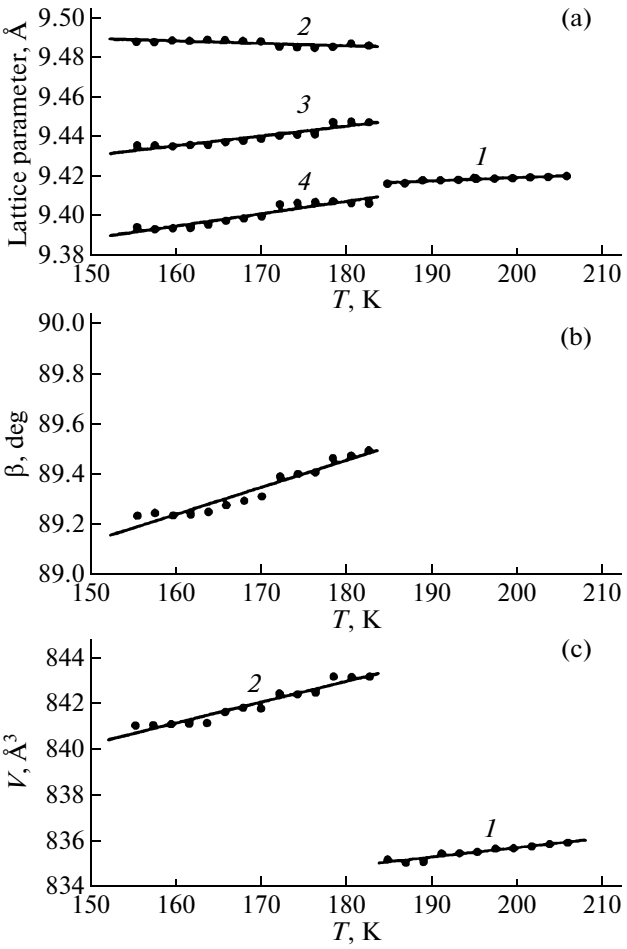

Fig. 6. Temperature dependences of the structural characteristics of the $(NH_4)_3Nb(O_2)_2F_4$ compound: (a) the unit cell parameters of (*1*) the cubic phase a_0 and (*2–4*) the monoclinic phase (*2*) $a_1\sqrt{2}$, (*3*) c_1, and (*4*) b_1; (b) the monoclinic angle β of the unit cell of the G_3 phase; and (c) the unit cell volumes of (*1*) the cubic phase G_0 and (*2*) the monoclinic phase G_3.

4. DISCUSSION OF THE RESULTS

The further consideration of the experimental data will be based on the works dealing with the group-theoretical analysis of the structural phase transitions in crystals with the space group $Fm\bar{3}m$ [12] and on the ISOTROPY [13] and ISODISPLACE [14] software packages.

At the first stage of our consideration, we determined the order parameters and the representations of the space group $Fm\bar{3}m$, which are involved in the phase transitions. For this purpose, we analyzed the permutation and mechanical representations [15] of the structures of the phases of the $(NH_4)_3Nb(O_2)_2F_4$ crystal. This analysis was carried out with the ISODISPLACE software package [14]. So, using the known structures of the cubic phase G_0 and the monoclinic phase G_3, we obtained the expansion of the orderings and displacements of the atoms involved in the $(NH_4)_3Nb(O_2)_2F_4$ crystal, which are transformed according to the irreducible representations of the space group $Fm\bar{3}m$. According to this analysis, the largest contributions to the distortion of the structure

Table 2. Atomic coordinates, isotropic thermal parameters (B_{iso}), and position occupancies (p) in the $(NH_4)_3Nb(O_2)_2F_4$ structure

Atom	p	X	Y	Z	B_{iso}, Å^2
			$T = 298$ K, $Fm\bar{3}m$		
Nb	1.0	0	0	0	3.22(4)
N1	1.0	1/2	1/2	1/2	3.5(2)
H1	0.5	0.557(2)	0.557(2)	0.557(2)	3
N2	1.0	1/4	1/4	1/4	4.3(1)
H2	1.0	0.190(1)	0.190(1)	0.190(1)	3
O	0.1667	0.197(1)	0.080(2)	0	5.2(4)
					$B_{iso} = 8(1)$
					$U_{11} = 0.012(1)$, Å^2
F	0.6667	0.2064(9)	0	0	$U_{22} = U_{33} = 0.032(1)$, Å^2
			$T = 133$ K, $P2_1/n$		
Nb	1.0	0.2930(4)	0.8735(3)	0.2386(3)	2.42(8)
F1	1.0	0.338(2)	0.877(1)	0.446(1)	3.2(2)
F2	1.0	0.581(2)	0.933(1)	0.236(1)	3.2(2)
F3	1.0	0.458(2)	0.7534(9)	0.245(1)	3.2(2)
F4	1.0	0.075(2)	0.7744(9)	0.319(1)	3.2(2)
O1	1.0	0.186(3)	0.818(1)	0.061(2)	5.1(3)
O2	1.0	0.238(3)	0.018(1)	0.263(2)	5.1(3)
O3	1.0	0.048(3)	0.960(1)	0.265(2)	5.1(3)
O4	1.0	0.329(3)	0.893(2)	0.033(2)	5.1(3)
N1	1.0	0.698(2)	0.137(1)	0.271(2)	3.3(2)
H1*a*	1.0	0.584(2)	0.137(1)	0.271(2)	3.3(2)
H1*b*	1.0	0.812(2)	0.137(1)	0.328(2)	3.3(2)
H1*c*	1.0	0.699(2)	0.192(1)	0.215(2)	3.3(2)
H1*d*	1.0	0.699(2)	0.082(1)	0.215(2)	3.3(2)
N2	1.0	0.210(2)	0.132(1)	0.003(2)	3.3(2)
H2*a*	1.0	0.102(2)	0.132(1)	0.948(2)	3.3(2)
H2*b*	1.0	0.321(2)	0.132(1)	0.947(2)	3.3(2)
H2*c*	1.0	0.210(2)	0.187(1)	0.058(2)	3.3(2)
H2*d*	1.0	0.210(2)	0.077(1)	0.058(2)	3.3(2)
N3	1.0	0.293(2)	0.620(1)	−0.014(2)	3.3(2)
H3*a*	1.0	0.280(2)	0.683(1)	0.020(2)	3.3(2)
H3*b*	1.0	0.184(2)	0.606(1)	0.935(2)	3.3(2)
H3*d*	1.0	0.301(2)	0.578(1)	0.061(2)	3.3(2)
H3*d*	1.0	0.406(2)	0.617(1)	0.933(2)	3.3(2)

are made by the following representations: Γ_5^+ (11–7) with the order parameter (η_1, η_1, η), Σ_2(4–2) with the order parameter (0, 0, 0, 0, 0, ξ, 0, $-\xi$, 0, 0, 0, 0), Σ_3(4–3) with the order parameter (0, 0, 0, 0, 0, ε, 0, ε, 0, 0, 0, 0), Γ_4^+ (11–9) with the order parameter (g_4, g_4, 0), and X_5^- (10–10) with the order parameter (x_5, 0, 0, 0, 0, 0). The parenthetic designations referring to the irreducible representations and the points of the Brillouin zone are given in accordance with the reference book [16].

Let us now consider the role of the aforementioned representations in the structural transformations in more details. As was already mentioned, the phase transitions occurring in the $(NH_4)_3Nb(O_2)_2F_4$ compound are transitions of the order–disorder type. Therefore, the representations responsible for the

Table 3. Characteristic bond lengths in the $(NH_4)_3Nb(O_2)_2F_4$ structure

298 K		133 K	
bond	length, Å	bond	length, Å
Nb–F	1.948(8)	Nb–F1	1.99(1)
		Nb–F2	2.07(1)
		Nb–F3	1.94(2)
		Nb–F4	2.09(1)
Nb–O	2.01(1)	Nb–O1	1.98(2)
		Nb–O2	1.97(1)
		Nb–O3	2.01(2)
		Nb–O4	1.98(2)
N1–F	2.771(9)	N1–F1	2.71(2)
		N1–F4	2.72(2)
		N1–F3	2.76(2)
		N1–F2	2.84(2)
N1–O	2.96(1)	N1–O4	2.91(3)
N2–F	3.361	N2–F2	2.78(2)
		N2–F3	3.08(2)
		N3–F4	2.82(2)
		N3–F2	2.86(2)
		N3–F1	3.06(2)
N2–O	2.90(1)	N2–O1	2.80(2)
		N2–O2	2.90(2)
		N3–O2	2.74
		N3–O1	2.81(2)
		N3–O3	2.88(2)

Table 4. Hydrogen bonds in the $(NH_4)_3Nb(O_2)_2F_4$ structure

A–H···*B* bond	H–*B* bond length, Å	*A*···*B* bond length, Å	*A*–H–*B* angle, deg
$T = 298$ K			
N2–H2···O	2.07(1)	2.897(6)	140.4(8)
N2–H2···F	2.54(1)	3.362(6)	141.2(7)
$T = 133$ K			
N1–H1*b*···F2	2.13(2)	2.83(2)	134(1)
N2–H2*a*···O1	2.03(2)	2.80(2)	142(1)
N2–H2*b*···O4	2.37(2)	3.10(2)	139(1)
N2–H2*b*···F2	2.03(2)	2.78(2)	139(1)
N2–H2*c*···F4	2.20(2)	2.92(2)	138(1)
N2–H2*c*···F3	2.33(2)	3.08(2)	140(1)
N2–H2*d*···O2	2.11(2)	2.90(2)	147(2)
N3–H3*a*···O1	1.94(2)	2.82(2)	164(1)
N3–H3*b*···F2	2.07(2)	2.87(2)	146(1)
N3–H3*b*···F1	2.32(2)	3.06(2)	140(1)
N3–H3*c*···O2	1.86(3)	2.74(3)	163(2)
N3–H3*d*···O3	2.11(3)	2.88(3)	143(2)
N3–H3*d*···F4	2.12(2)	2.82(2)	143(1)

phase transitions should be those resulting in an ordering of structural groups. The order parameter, which is transformed according to the irreducible representation Γ_4^+ (11–9), provides rotation of the $Nb(O_2)_2F_4$ polyhedron around the monoclinic axis **b** and does not lead to an ordering of any groups; therefore, this order parameter, most likely, is not a leading or critical parameter in the phase transitions. The representation X_5^- (10–10) is involved in the process of ordering of only the $Nb(O_2)_2F_4$ polyhedron; however, the contribution from this representation to the ordering of the structure is significantly less than that coming from the representations Γ_5^+ (11–7), Σ_2(4–2), and Σ_3(4–3). Consequently, the representation X_5^- (10–10) cannot be leading, at least, in the first phase transition occurring at the temperature $T_1 = 193.0$ K, because the appearance of the parameter transformed according to the representation X_5^- is accompanied by the change in the translational symmetry and by the appearance of superstructure reflections. However, no appearance of superstructure reflections is observed in the X-ray diffraction patterns down to the temperature of the third phase transition T_3. In addition, this order parameter and the corresponding representation do not describe the translational symmetry of the monoclinic phase G_3. Thus, we can consider that the experimentally established fact is that the representation Γ_5^+ (11–7) and all the parameters related to it are critical in the first phase transition ($T_1 = 193.0$ K). The further sequence of the order parameters of the representations Σ_2 and Σ_3 cannot be established yet. Here, we can only suggest a probable sequence of occurrences of the critical representations. However, the ordering of the NH_4 ion is associated only with the representation Σ_3. Since the ammonium ion as the lightest element in the structure is likely to be ordered in the last, the sequence of occurrences of the critical representations is as follows: Γ_5^+ (at $T_1 = 193.0$ K), Σ_2 (at $T_2 = 187.2$ K), and Σ_3 (at $T_3 = 185.4$ K). Now, using this information, we can obtain symmetries of the intermediate stages. Table 5 presents the relationships between the components of the phenomenological order parameters, information about the symmetries of the phases of the $(NH_4)_3Nb(O_2)_2F_4$ compound, and the relationships between the principal translations of the unit cells of the parent cubic and distorted phases.

Thus, the changes in the point and translational symmetry, which are indicated by the splitting of structural reflections and by the positions of the super-

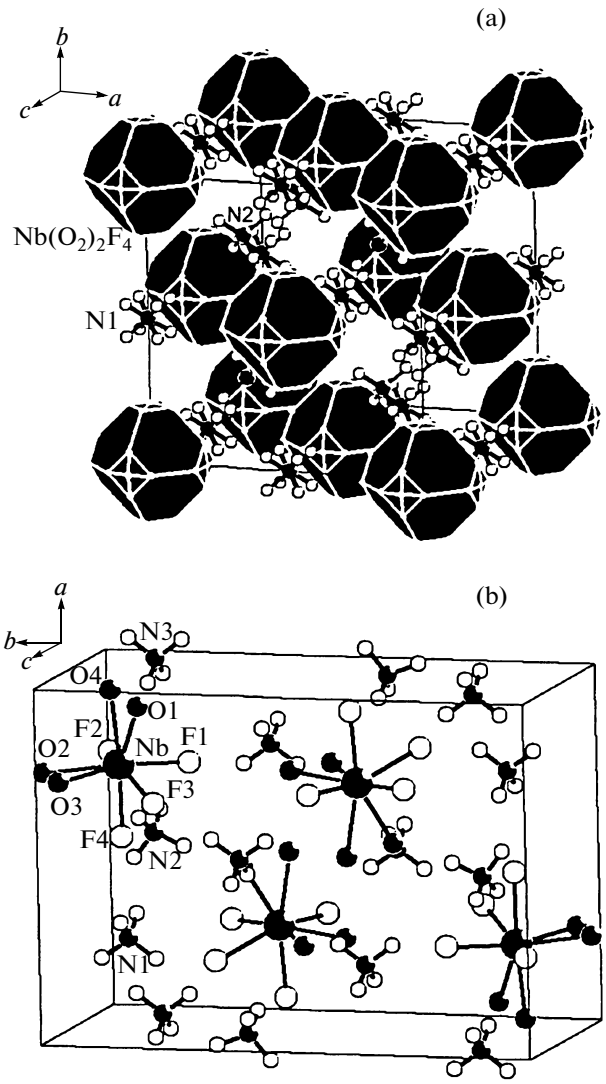

Fig. 7. Structures of the phases of the $(NH_4)_3Nb(O_2)_2F_4$ compound: (a) the cubic phase G_0 at a temperature $T =$ 298 K and (b) the monoclinic phase G_3 at a temperature $T = 133$ K.

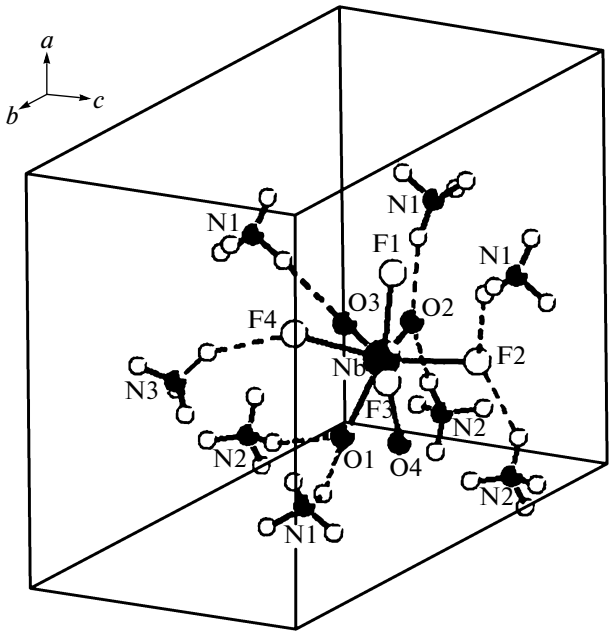

Fig. 8. System of hydrogen bonds in the structure of the $(NH_4)_3Nb(O_2)_2F_4$ compound in the monoclinic phase G_3.

structure reflections of the G_3 phase in the X-ray diffraction patterns, can be described by the interaction of three phenomenological order parameters so that one of these order parameters is transformed according to the irreducible representation Γ_5^+ (11–7) of the space group $Fm\bar{3}m$ with the wave vector Γ at the center of the Brillouin zone (the wave vector $\mathbf{k}_{11} = (0, 0, 0)$) and the other two order parameters are transformed according to the representations $\Sigma_2(4–2)$ and $\Sigma_3(4–3)$ with the wave vector $\mathbf{\Sigma}$ at the point located inside the Brillouin zone (the wave vector $\mathbf{k}_4 = (1/2, 1/2, 0)$). These order parameters, which specify the symmetry of the distorted phase, are referred to, in accordance with [17], as the critical order parameters. The structural distortions, atomic displacements, and atomic orderings, which are related to the critical order parameter, are also referred to as critical.

Although the symmetries and structures of the intermediate phases G_1 and G_2 cannot yet be established experimentally, we will make an attempt to describe the processes occurring in these compounds.

Since the greatest contribution to the total entropy of the phase transitions comes from the first phase transition occurring at the temperature $T_1 = 193.0$ K [8], the leading role played in this transition should be given to the $Nb(O_2)_2F_4$ group, which is disordered in the cubic phase to a greater extent as compared to the tetrahedral ammonium groups NH_4. Next, we will simulate the ordering of the $Nb(O_2)_2F_4$ polyhedron, which, according to the structure of the low-temperature phase G_3, has the symmetry corresponding to $2mm(C_{2v})$. The simulation will be performed by analogy with the procedure used in our recent works [3, 5]. The $Nb(O_2)_2F_4$ polyhedron can be represented as a vector directed from the center of the rectangle built up on the $(O_2)_2$ atoms to the center of mass of the F atoms. In the cubic unit cell, the $Nb(O_2)_2F_4$ octahedron is oriented in such a way (Fig. 10) that this vector has the coordinates $(x, x, 0)$; i.e., it is in the position $48h$ of the face-centered cubic unit cell. By replacing the polyhedron with the vector, it is easy to obtain the number of different orientations of the $Nb(O_2)_2F_4$ octahedron in the cubic phase. Since the $(x, x, 0)$ position in the cubic phase has a multiplicity of 48, the number of orientations of the $Nb(O_2)_2F_4$ octahedron

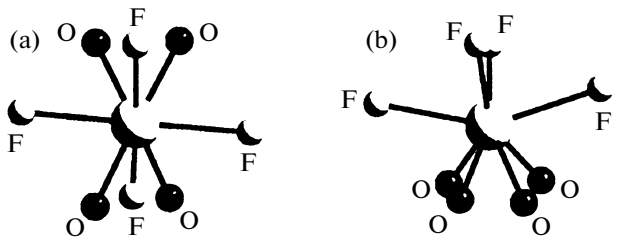

Fig. 9. A view of the $Nb(O_2)_2F_4$ polyhedron in the structure of the $(NH_4)_3Nb(O_2)_2F_4$ compound in the monoclinic phase G_3 in two projections: (a) the top view and (b) the side view.

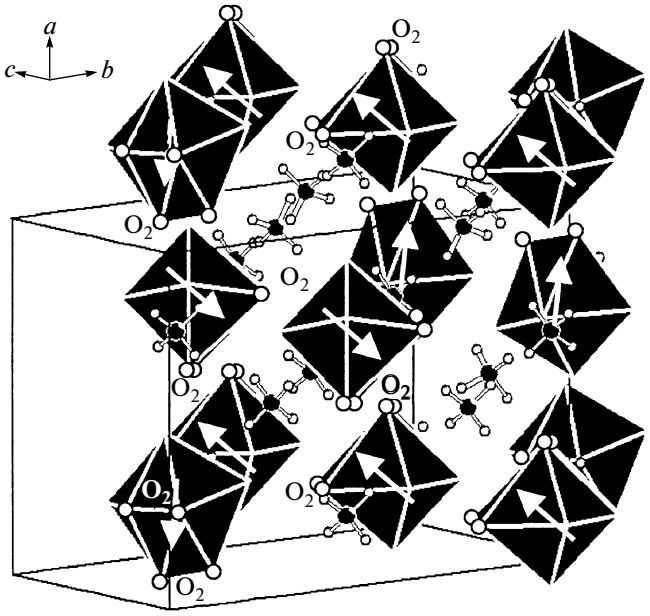

Fig. 10. Pseudocubic structure of the $(NH_4)_3Nb(O_2)_2F_4$ compound in the atomic coordinates of the monoclinic phase G_3: O_2 is the dumbbell of the peroxide group $(O_2)^{2-}$, and the white arrows represent the vectors connecting the center of mass of the $(O_2)_2$ group and the center of mass of four F atoms in each $Nb(O_2)_2F_4$ polyhedron.

in a particular site is $N_0 = 48/Z = 48/4 = 12$, where $Z = 4$ is the number of formula units in the face-centered cubic unit cell. Thus, in the cubic phase, there are 12 differently oriented $Nb(O_2)_2F_4$ polyhedra or the vectors replacing the $Nb(O_2)_2F_4$ group (Figs. 10 and 11).

By using the group-theoretical analysis of the permutation representation, it is easy to determine how the occupancies of these twelve positions change with variations in the symmetry and, consequently, to elucidate which of the orientations of the polyhedron can occur with a higher probability or can be energetically more favorable after the phase transition when the critical order parameter is known. For these purposes, it is most convenient to use the ISODISPLACE software package [14], because it visualizes the obtained result.

Figure 11 schematically illustrates the ordering of the $Nb(O_2)_2F_4$ polyhedron during the phase transitions $Fm\bar{3}m \longrightarrow C2/m \longrightarrow P2_1/n$ without one intermediate phase, i.e., $P2_1/m$. We omit the information about this phase, because the question as to the sequence of occurrences of the representations Σ_2 and Σ_3 in this compound still remains open. It can be seen

Table 5. Symmetries of the $(NH_4)_3Nb(O_2)_2F_4$ phases and relationships between the phenomenological order parameters and the entropies of the phase transitions

Characteristic	$T > 193$ K	$193 \le T < 187$ K	$187 \le T < 185$ K	$T \le 185$ K
Critical representations and order parameters	–	$\Gamma_5^+(11-7)$ (η_1, η_1, η)	$\Gamma_5^+(11-7)$ (η_1, η_1, η) + $\Sigma_2(4-2)$ $(0, 0, 0, 0, 0, \xi, 0, -\xi, 0, 0, 0, 0)$	$\Gamma_5^+(11-7)$ + $\Sigma_2(4-2)$ $(0, 0, 0, 0, 0, \xi, 0, -\xi, 0, 0, 0, 0)$ + $\Sigma_3(4-3)$ $(0, 0, 0, 0, 0, \varepsilon, 0, \varepsilon, 0, 0, 0, 0)$
Space group	$Fm\bar{3}m$	$C2/m$	$P2_1/m$	$P2_1/n$
$\mathbf{a}_i$	$\mathbf{a}_0$	$(-\mathbf{a}_0 + 2\mathbf{b}_0 - \mathbf{c}_0)/2$	$(\mathbf{a}_0 + \mathbf{c}_0)/2$	$(-\mathbf{a}_0 - \mathbf{c}_0)/2$
$\mathbf{b}_i$	$\mathbf{b}_0$	$(-\mathbf{a}_0 + \mathbf{b}_0)/2$	$\mathbf{a}_0 - \mathbf{b}_0$	$\mathbf{a}_0 - \mathbf{c}_0$
$\mathbf{c}_i$	$\mathbf{c}_0$	$(\mathbf{a}_0 + \mathbf{b}_0)/2$	$\mathbf{b}_0$	$-\mathbf{b}_0$
V_i/V_0	1	1	4	4
Z_i	4	2	1	1

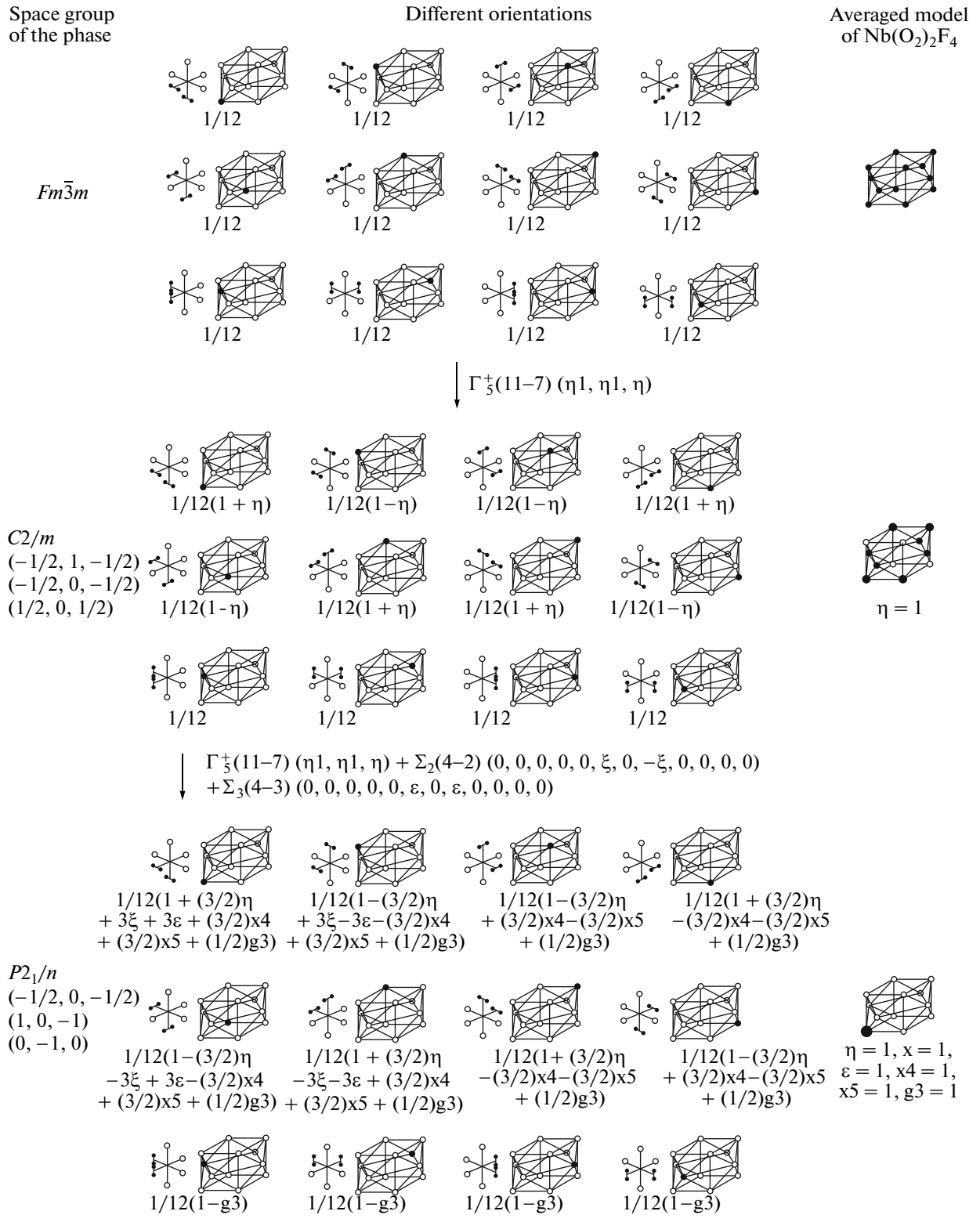

Fig. 11. Model of the ordering of the $Nb(O_2)_2F_4$ polyhedra in the C_{2v} configuration (see Fig. 1). Numbers under the particular orientation of the polyhedron indicate the probability of its existence; η, ξ, and ε are the components of the critical order parameters, which are transformed according to the Γ_5^+, Σ_2, and Σ_3 representations, respectively; and x_4, x_5, and g_3 are the components of the noncritical order parameters, which are transformed according to the X_4^-, X_5^-, and Γ_3^+ representations, respectively.

from the picture of the ordering that the aforementioned critical order parameters do not provide a complete ordering of the $Nb(O_2)_2F_4$ polyhedron in the monoclinic phase. However, the structure of this phase indicates that all $Nb(O_2)_2F_4$ polyhedra are completely ordered.

Now, it is appropriate to note that, in a number of cases, the distortion of the structure of the parent phase cannot be described only by the critical order parameters. In the distorted (disymmetric) phase, there can occur atomic displacements or atomic orderings that are compatible with the symmetry of this phase and which are specified by the noncritical (secondary) order parameters and irreducible representations. The entire set of order parameters, both critical and noncritical, which appear during the phase transition, forms the complete order parameter condensate [17]. The noncritical distortions have a secondary character and are insignificant in the vicinity of the phase transition points.

Apart from the critical order parameters (the representations Γ_5^+(11–7), Σ_2(4–2), and Σ_3(4–3)), the noncritical order parameters (the representations X_4^-, X_5^-, Γ_3^+) are also involved in the process of ordering of the $Nb(O_2)_2F_4$ polyhedron and make an additional contribution to this ordering, so that the action of the latter order parameters leads to a complete ordering of $Nb(O_2)_2F_4$ (Fig. 11), which corresponds to that obtained in the experiment. It should be noted that the total entropy of the ordering of this structural element is equal to $R\ln 12$.

The ordering of the ammonium ion is schematically illustrated in Fig. 12. The entropy of the ordering of this structural element is equal to $R\ln 12$; therefore, the total entropy of the phase transitions is $\Delta S = R\ln 12 + R\ln 2 = R\ln 24$, which is very close to the experimentally measured value $R\ln 20$. The slightly smaller value of the experimentally measured entropy of the phase transitions can be explained by the fact that, after three phase transitions, the $Nb(O_2)_2F_4$ polyhedron remains disordered, and a further ordering occurs as the difference between the temperature of the sample and the temperature of the phase transition increases with an increase in the noncritical order parameters.

The phase transition is accompanied by the displacements of the atoms Nb, N1, N2, and N3 with respect to the positions in the cubic unit cell (the components of all the atomic displacements in the distorted phases are given with respect to the axes of the former cubic unit cell):

$$\Delta\mathbf{r}(\text{Nb}) = (-0.220, 0.108, -0.189)\ \text{Å},$$
$$\Delta\mathbf{r}(\text{N1}) = (-0.240, 0.141, -0.165)\ \text{Å},$$
$$\Delta\mathbf{r}(\text{N2}) = (-0.120, 0.004, -0.255)\ \text{Å},$$
$$\Delta\mathbf{r}(\text{N3}) = (-0.131, 0.210, -0.322)\ \text{Å}.$$

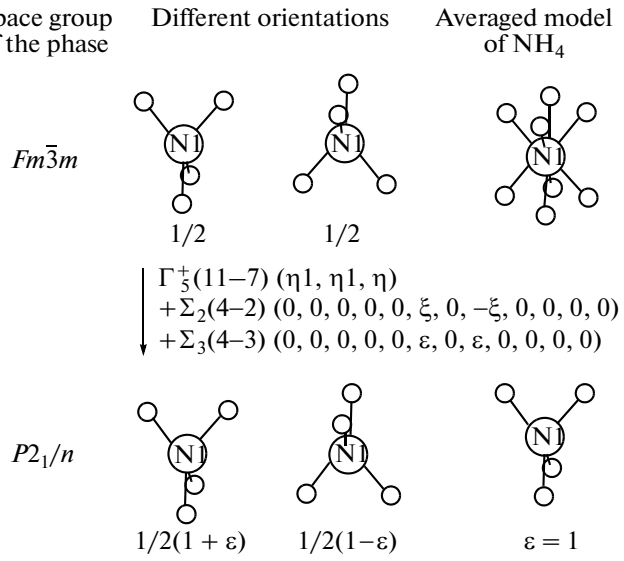

Fig. 12. Model of the ordering of the NH_4 polyhedron in the position 4*b*. Numbers under the particular orientation of the polyhedron indicate the probability of its existence; η is the component of the critical order parameters, which is transformed according to the Σ_3 representation.

The contribution to the displacements of all these atoms is provided by the following representations: Γ_4^+, Γ_5^+, X_5^-, Σ_2, and Σ_3. However, the largest displacement is provided by the contribution from the representation Σ_2. The contribution from the representation Σ_3 to the atomic displacement is approximately two times smaller than the contribution from the representation Σ_2. In this case, the atoms are displaced along the **a** axis of the monoclinic unit cell. The contribution from the representations Γ_4^+, Γ_5^+, and X_5^- to the atomic displacement is one order of magnitude smaller than the contribution from the above-considered representations Σ_2 and Σ_3.

From the physical point of view, the phase transitions can be interpreted as follows. During cooling in the first phase transition, there occurs a partial ordering of the $Nb(O_2)_2F_4$ polyhedron under the action of the critical representation Γ_5^+, which provides the formation of hydrogen bonds (Table 4) with the already existing ordered ammonium N2 ions. In the second phase transition with the critical representation Σ_2, the $Nb(O_2)_2F_4$ anion continues to undergo a partial ordering, and the number of hydrogen bonds increases. At the same time, the process of rotation of the $Nb(O_2)_2F_4$ polyhedron begins to occur under the action of the noncritical representation Γ_4^+ due to the already existing hydrogen bonds, which tent to improve their own geometrical characteristics. The number of hydrogen bonds increases, and their influ-

ence is enhanced. In the third phase transition, the $Nb(O_2)_2F_4$ polyhedron becomes completely ordered; in this case, the $Nb(O_2)_2F_4$ anion has the maximum number of hydrogen bonds (equal to 12) with the ordered ammonium N2 and N3 ions. The disordered ammonium N1 ion undergoes ordering and forms one hydrogen bond with $Nb(O_2)_2F_4$ (Table 4). The processes of rearrangement are fully completed.

5. CONCLUSIONS

Thus, using X-ray powder diffraction in combination with the appropriate procedures of the symmetry analysis of the complete order parameter condensate, we have determined the structural transformations occurring during the phase transitions observed in the $(NH_4)_3Nb(O_2)_2F_4$ crystal, which can be schematically represented in the following form:

$$Fm\bar{3}m \xrightarrow[(\eta 1, \eta 1, \eta)]{\Gamma_5^+(11-7)} C2/m \xrightarrow[(\eta 1, \eta 1, \eta)(0, 0, 0, 0, 0, \xi, 0, -\xi, 0, 0, 0, 0)]{\Gamma_5^+(11-7) \otimes \Sigma_2(4-2)} P2_1/m$$
$$\xrightarrow[(\eta 1, \eta 1, \eta)(0, 0, 0, 0, 0, \xi, 0, -\xi, 0, 0, 0, 0)(0, 0, 0, 0, 0, \varepsilon, 0, \varepsilon, 0, 0, 0, 0)]{\Gamma_5^+(11-7) \otimes \Sigma_2(4-2) \otimes \Sigma_3(4-3)} P2_1/n.$$

ACKNOWLEDGMENTS

The authors would like to thank Professor V.I. Zinenko and Professor I.N. Flerov for helpful discussions of the results obtained in this work and Senior Researcher N.M. Laptash for providing the samples used in our experiments and for a number of comments that have significantly improved the content of this paper.

This study was supported by the Russian Foundation for Basic Research (project no. 09-02-00062) and the Council on Grants from the President of the Russian Federation for Support of Leading Scientific Schools of the Russian Federation (grant no. NSh-4645.2010.2).

REFERENCES

1. I. N. Flerov, M. V. Gorev, K. S. Aleksandrov, A. Tressaud, J. Grannec, and M. Couzi, Mater. Sci. Eng., R **24** (3), 81 (1998).
2. J. Ravez, G. Peraudeau, H. Arend, S. C. Abrahams, and P. Hagenmuller, Ferroelectrics **26**, 767 (1980).
3. M. S. Molokeev, S. V. Misyul', V. D. Fokina, A. G. Kocharova, and K. S. Aleksandrov, Phys. Solid State **53** (4), 834 (2011).
4. K. S. Aleksandrov, S. V. Misyul, M. S. Molokeev, and V. N. Voronov, Phys. Solid State **51** (12), 2505 (2009).
5. M. S. Molokeev and S. V. Misyul', Phys. Solid State **53** (8), 1672 (2011).
6. Ž. Ružić-Toroš, B. Kojić-Prodić, and M. Šljukić, Inorg. Chim. Acta **86** (3), 205 (1984).
7. Von R. Schmidt, G. Pausewang, and M. Massa, Z. Anorg. Allg. Chem. **488**, 108 (1982).
8. V. D. Fokina, A. F. Bovina, E. V. Bogdanov, E. I. Pogorel'tsev, N. M. Laptash, M. V. Gorev, and I. N. Flerov, Phys. Solid State **53** (10), 2147 (2011).
9. V. I. Mikheev, *X-Ray Determinant of Minerals* (Geologiya i Okhrana Nedr, Moscow, 1957) [in Russian].
10. J. W. Visser, J. Appl. Crystallogr. **2**, 89 (1969).
11. L. A. Solovyov, J. Appl. Crystallogr. **37**, 743 (2004).
12. K. S. Aleksandrov, S. V. Misyul, and E. E. Baturinets, Ferroelectrics **354**, 60 (2007).
13. H. T. Stokes, D. M. Hatch, and B. J. Campbell, *Isotropy: A Program Which Displays Information About Space Groups, Irreducible Representations, Isotropy Subgroups, and Phase Transitions* (Brigham Young University, Provo, Utah, United States, 2007); stokes.byu.edu/isotropy.html.
14. B. J. Campbell, H. T. Stokes, D. E. Tanner, and D. M. Hatch, J. Appl. Crystallogr. **39**, 607 (2006).
15. Yu. A. Izyumov and V. N. Syromyatnikov, *Phase Transitions and Crystal Symmetry* (Nauka, Moscow, 1984; Kluwer, New York, 1990).
16. O. V. Kovalev, *Irreducible and Induced Representations and Co-Representations of Fedorov's Groups* (Nauka, Moscow, 1986) [in Russian].
17. V. P. Sakhnenko, V. M. Talanov, and G. M. Chechin, Fiz. Met. Metalloved. **62** (5), 847 (1986).

Translated by O. Borovik-Romanova